AIAA 2001-0084
Asymmetry Effects in Numerical Simulation of Supersonic Flows with Upstream Separated Regions

C.G. Rodriguez
National Research Council, Hampton, VA

39th AIAA Aerospace Sciences Meeting & Exhibit
8-11 January 2001 / Reno, NV

ASYMMETRY EFFECTS IN NUMERICAL SIMULATION OF SUPERSONIC FLOWS WITH UPSTREAM SEPARATED REGIONS

C.G. Rodriguez*

National Research Council, Hampton, VA 23681

Abstract

The present paper studies the numerical simulation of flows with shock/boundary-layer upstream interaction, under conditions of symmetry in geometry, boundary conditions, and grid. For this purpose, a series of two- and three-dimensional numerical test-cases were carried out. The tests showed that standard numerical schemes, which appear to be symmetry-preserving under most flow configurations, produce non-symmetric perturbations when large separated regions are present. These perturbations are amplified when the core flow is under compression. If the flow-blockage due to separation is sufficiently large, the symmetry of the flow may collapse altogether. Experimental evidence of this numerical behavior is also considered.

Nomenclature

H	test-section inlet height [m]
k	turbulence kinetic energy $[m^2/s^2]$
M	Mach number
p	pressure [Pa]
T	temperature [°K]
V	velocity [m/s]
x	axial (streamwise) coordinate [m]
y	vertical coordinate [m]
y^+	dimensionless vertical turbulence coordinate
z	lateral coordinate [m]
μ	viscosity $[N\ s/m^2]$
ρ	mass density $[kg/m^3]$
ω	specific dissipation rate [1/s]

Subscripts:

0	total conditions
back	back (exit) conditions
exit	exit conditions
inlet	inlet conditions
j	injectant (jet) conditions
s	static conditions

1. Introduction

In a previous paper[1] the author and co-workers reported an unexpected numerical behavior in the simulation of dual-mode scramjet combustors. Under conditions of perfect symmetry in geometry, grid and boundary conditions, computational fluid dynamic (CFD) calculations showed an asymmetric response when a shock-train/separated-flow system was present in the flowfield. Other researchers using a completely different computational methodology reported similar results[2].

The problem under consideration is shown in figure 1, which depicts the transverse plane of a flow in a rectangular cross-section duct. A supersonic incoming flow is subjected to an adverse pressure-gradient due to a back-pressure p_{exit}; the source of this pressure could be, for example, a combustion process or a diffuser. In general, for any p_{exit} between inlet and normal-shock values the flow configuration will be a confined, compressed core-

---

* Research Associate, Member AIAA

flow surrounded by separated regions[3]. The separating boundary-layer creates a series of shocks, or shock train, that further compresses the core flow. This shock-train will be mainly oblique or normal, depending on whether the exit Mach is supersonic or subsonic. Since the shock-train/separated flow interaction propagates upstream of the source of pressure, the whole phenomenon is referred to as 'upstream interaction'. The symmetry and stability of flows with upstream interactions is the focus of the present paper.

There exists experimental evidence to suggest that these flows may not remain symmetric. Carroll[4] and Carroll and Dutton[5] reported a series of experiments on supersonic rectangular ducts subjected to adverse pressure-gradients. They were able to create an upstream interaction similar to the one depicted in figure 1. At low Mach numbers (M ~ 1.60) the flow appeared to be mostly symmetric. At high Mach numbers (M ~ 2.50), however, the schlieren visualization and pressure traces showed a large degree of asymmetry, similar to the one reported in reference 1.

Asymmetrical behavior under symmetry conditions have been previously reported for other types of flow. Levy et al[6] did so for flows around slender bodies at high angles of attack (AOA). Experimentally, these flows show a convective instability mechanism, i.e., minute imperfections can cause large flow asymmetries which vanish when the disturbance is removed. The authors contended that "numerical simulation of such flows should give the basic symmetric solution as long as algorithms, boundary and initial conditions, and grids are perfectly symmetric". They showed that the left-hand-side of some implicit time-integration algorithms could create asymmetries in the steady-state solution. In particular, the diagonal approximate-factorization (DAF) algorithm of Pulliam and Chaussee[7] was shown not to be symmetry-preserving. For low AOA the effects were small, the flowfield appearing largely symmetric. At high AOA, however, the flowfield was manifestly asymmetric. Furthermore, the asymmetry did not correlate with the experimentally-observed pattern.

There may be some analogy between external flows around high-AOA slender bodies, and internal flows with upstream interaction. The duct flows at low Mach numbers would resemble the low-AOA bodies, with the flow largely symmetric; the asymmetry of high-Mach duct-flows would be similar to that of high-AOA bodies. Unlike the slender-body experiment, the asymmetry in the duct flows could not be traced to any known perturbation. This would indicate a more fundamental instability than the convective type of the slender-body flows.

The present paper will attempt to determine the nature of the numerical asymmetry observed in flows with upstream interaction. First, a series of two-dimensional numerical tests will be carried out to determine the possibility of obtaining a basic symmetric solution for flows with upstream interaction. Next, three-dimensional effects will be studied in a rectangular-section duct. Finally, the experiment of Carroll and Dutton will be modeled to compare numerical asymmetries with experimental ones.

2. Computational Approach

All calculations presented in this paper were done with NASA Langley's VULCAN code. This code has been extensively described before[8]. Only the specific implementation used in this paper will be detailed here.

The inviscid fluxes were modeled with Edwards' low-dissipation flux-split scheme[9]. Fluxes were evaluated either with a first-order approximation, or with a third-order MUSCL scheme and Van Leer's flux limiter.

The full viscous fluxes were modeled with second-order central differences. In all cases, viscous flows were assumed fully-turbulent. Wilcox' 1998 k-ω turbulence model was used, with Wilcox' wall-matching functions at solid walls[10].

In all cases, the flow was assumed to be spatially-elliptic. The gas was modeled as calorically-perfect air. Time-integration was done with either a two-step explicit Runge-Kutta (RK) scheme, or the implicit diagonal approximate-factorization (DAF).

All calculations were run in double-precision on 64-bit machines (Cray c90, Origin 2000, SGI R10000)

3. Two-Dimensional Numerical Tests

A series of two-dimensional numerical test cases were devised to establish the existence of a numerical scheme that could produce a basic symmetric solution for flows with upstream interaction. Each case would try to isolate or add elements present in these flows, and determine their effect on the symmetry of the solution. The tests were based on the conditions for the Carroll and Dutton experiment[5]. The inlet conditions (assumed uniform for all cases) were M = 2.50, p_0 = 310 KPa and T_0 = 295 °K. The inlet height was H = 0.0381 m (used to non-dimensionalize lengths in all plots for this section).

In all cases, inviscid fluxes were modeled as first-

order, in order to find the simplest algorithm that would be symmetry-preserving. Unless otherwise noted, all wall conditions were no-slip adiabatic and supersonic extrapolation was imposed at the exit.

3.1. Convergent Duct

Figure 2 shows a convergent duct, which is reminiscent of the core flow in figure 1. The main purpose of the test is to produce a shock train similar to the one observed in upstream interaction but without any separated flow being present. This would allow a preliminary determination on the symmetry-preserving properties of a given algorithm. The grid is symmetric with respect to $y = 0$. Its dimensions are 177×81 (streamwise $\times$ height). All results to be shown for this case were considered converged after the L_2-norm of the residual decreased four orders of magnitude.

The Mach contours obtained using RK integration and assuming inviscid flow are presented in figure 3-a); a series of shocks can be seen, similar to the shock train in the core-flow of figure 1. The flow appears symmetric and this is confirmed by the streamwise variation of the vertical velocity component at the symmetry plane, V_y ($y = 0$) (figure 3-b): the distribution is mostly noise, without any apparent correlation with the flowfield. Adding the viscous fluxes (figure 4) produces a qualitatively similar flowfield; the resulting scheme also appears to be symmetry-preserving.

Integrating the inviscid flow with the DAF scheme shows a Mach-number pattern virtually identical to that of the RK method (figure 5-a), but now V_y ($y = 0$) is no longer noise (figure 5-b). Its distribution is several orders of magnitude bigger than that of the RK scheme, and it correlates with the flowfield; in particular, the two peaks correspond to the shocks intersecting the symmetry line. This behavior of the DAF scheme agrees with the findings of Levy et al[6].

This simple test seems sensitive enough to capture the symmetry-preserving behavior of an algorithm, and suggests that at least first-order space-integration with the RK time-integration is symmetry preserving. It would also indicate that, by itself, a shock-train is not a fundamental source of asymmetry.

3.2. Sudden-Expansion Duct

Figure 6 shows the layout of a duct with a sudden expansion or backward-facing step. This domain will be used to generate a shock-train/boundary-layer interaction. This can be accomplished two ways: by injecting air at a pressure p_{inj} and very low speed (as shown in the figure), or by applying a back-pressure p_{back} at the exit. Either proce-

dure can create a shock/separated-flow interaction, whether upstream or not. Injection makes it easier to control the interaction at low or moderate compression in the core flow; back-pressure is better suited for high compression. As will be seen, the degree of core-flow compression will have an effect on the symmetry of the flow. Unless otherwise noted the grid dimensions are 153×161 (inlet or isolator) and 201×201 (expansion).

Figure 7 presents the results for $p_{inj} = 40$ KPa, using the RK scheme. The isolator has been shortened to reduce computational effort and its grid has dimensions 53×161. These calculations were converged six orders of magnitude. The Mach contour-plot (figure 7-a) shows an oblique shock-train interacting with the separated flow produced by the injection. The core-flow exit-pressure is slightly larger than the inlet pressure (about 20 KPa). The flowfield appears symmetric, but the centerline normal-velocity distribution (figure 7-a) is greater than machine-zero and correlated to the flow. The results obtained using the DAF scheme are virtually identical (figure 8), except for the fact that the centerline perturbations are an order of magnitude bigger.

Increasing the injectant pressure to $p_{inj} = 95$ KPa produces substantial upstream interaction, as can be seen in figure 9 (after converging six orders). The core-flow exit pressure turns out to be twice as large as the inlet pressure, indicating a higher core-flow compression with respect to the previous case. Apparently as a result, the velocity perturbation generated with the RK scheme has increased by two orders of magnitude. When using the DAF scheme (figure 10), the flow symmetry collapses altogether.

Figure 11 shows the results (converged four orders) when the upstream interaction is brought about by applying a back-pressure at the exit; in this case, $p_{back} = 80$ KPa, or about four times the inlet pressure (and approximately twice the core-flow compression of the previous case). As can be seen, the flow symmetry collapses regardless of the numerical scheme (RK or DAF) used. For comparison, figure 12 shows what the flowfield would look like if only half of the duct height had been solved, with a symmetry assumption imposed at the centerline. Not only the flow is symmetric, but the extent of the upstream interaction into the isolator is about half as much as in the previous case.

3.3. Analysis

From the previous series of numerical tests, some preliminary conclusions may be drawn:

• The presence of large separated-flow regions interacting with shock-trains appears to be the immediate source of

asymmetric perturbations greater than machine-zero.

• These perturbations are present even with numerical schemes that appear to be symmetry-preserving when applied to more conventional flows.

• The asymmetries are either introduced numerically (by the scheme or the modelization itself), or are inherent to flows with large shock/separation interaction.

• If the latter is true, a basic symmetric solution (i.e., symmetric within machine zero) for these flows may not be possible with conventional computational techniques

• Regardless of their origin, asymmetric perturbations seem to increase with the core-flow compression.

• Flows that are that are under relatively high compression appear to be unstable, i.e., any perturbation will be amplified until the flow-symmetry collapses regardless of the scheme used.

• The extent of the upstream interaction appears to be larger when the flow symmetry is allowed to collapse, than when the symmetry is imposed as boundary condition.

4. Three-Dimensional Numerical Test

To determine the numerical stability of three-dimensional flows, a duct with rectangular cross-section was tested; it is based on the isolator section of the experimental scramjet modeled in reference 1. Figure 13 shows the layout of the duct, with the two symmetry planes also drawn. The duct height was H = 0.032 m (used to non-dimensionalize all plots in this section). Inlet nominal conditions were M = 2.50, p_0 = 1.0 MPa and T_0 = 2000 °K. To promote the existence of upstream interaction, an incoming boundary-layer profile was imposed at the inlet. A step-wise uniform back-pressure distribution was applied at the exit: a value of 150 KPa was used a small distance from the sidewalls, and 250 KPa elsewhere in the section. It was hoped this distribution would recreate the expected flowfield of a dual-mode scramjet. For qualitative purposes a coarse grid of dimensions 101 × 25 × 125 (streamwise × height × width) was used. The numerical scheme consisted of third-order fluxes with DAF time integration. Since the flow is highly compressed (exit pressure was four times the inlet for the most part), a symmetry-preserving algorithm was not deemed necessary.

The overall flowfield configuration can be seen in figure 14. A central separated-flow region, similar to the two-dimensional case, is clearly visible. Separation adjacent to the sidewalls is also apparent. The Mach contour-plot in the vertical symmetry-plane (figure 15-a) shows that flow symmetry has collapsed, just like in the two-dimensional case. In the horizontal symmetry-plane (figure 15-b), symmetry has

also been lost, but not to the same extent as in the vertical plane. This may be due to the fact that flow blockage from separation is smaller in the horizontal plane than in the vertical. If this is the case, it may suggest that the stability of the flow-symmetry depends, for a given amount of compression, on the 'slenderness' of the core flow with respect to the geometric duct: the narrower the core-flow relative to the relevant duct dimension, the more likely the flow will depart from symmetry or its symmetry collapse altogether.

5. Experimental Test Case

The results from the previous sections showed that asymmetry is associated with flows containing upstream interaction, and with highly-compressed, slender core-flows. This asymmetry will now be compared with the one observed experimentally in the series of experiments carried out by Carroll and Dutton[5]. Their full description may be found in the references cited previously; only a brief outline will be presented here, followed by the numerical results.

5.1. Description of the Experiment

The schematic of the supersonic wind-tunnel facility is shown in figure 16. The wind tunnel can be divided in four sections, in downstream order: a constant-area stagnation chamber; a convergent-divergent nozzle; a test-section with divergent walls; and an exit diffuser. The entire facility is symmetric, and the cross-section, rectangular with constant width. For the nominal test M_{inlet} = 2.50, the inlet height is H = 0.0381 (which again was used for non-dimensionalization of the results); the section aspect-ratio is 2. The top and bottom walls have a divergence angle of 0.25 deg. The operating conditions are p_0 = 310 KPa and T_0 = 295 °K.

Figure 17 presents experimental oil and schlieren visualizations, for a diffuser geometry such that the test-section exit back-pressure is p_{exit}/p_0 = 0.374. The oil visualizations correspond to the top and bottom surfaces, while the schlieren provides a side view. The asymmetry of the flow is evident. Following the terminology of the researchers, the flow is said to be "attached" to the lower wall and "separated" from the top wall (even though separation is apparent in both walls). Note also the three-dimensionality of the flow, with corner recirculation possibly due to the presence of secondary flows. There appears to be a slight asymmetry in the horizontal plane, especially on the top surface.

5.2. Numerical Results

The test was approximated with a two-dimensional assumption. The stagnation and nozzle sections were solved first, and the exit conditions from the nozzle were used as inlet conditions for the test section. Each domain was solved elliptically using third-order inviscid fluxes and the DAF scheme. Since it is expected for this flow to be unstable, the DAF scheme was chosen to allow high CFL numbers. Convergence was assumed when the wall-pressure traces remained essentially unchanged.

The grid used for the stagnation and nozzle domain is shown in figure 18, with an expanded view of the nozzle. Only half of the domain was solved, with a grid of dimensions 435×101. The inlet conditions were subsonic, and extrapolation was used at the exit. A symmetry condition was imposed at the top, and no-slip adiabatic was assumed at the wall. For this domain no wall-functions were used, the boundary-layer being integrated to the wall; the resulting y^+ had a maximum value of about 1 at the throat. Calculations were converged four orders of magnitude. The resulting Mach contours can be seen in figure 19.

The computational domain for the test section extended to its entire length, $l_{test}/H = 20$. The exit diffuser was represented by a mixed subsonic/supersonic exit boundary condition, with the experimental pressure applied there. The baseline grid had dimensions 801×161. The grid was clustered in the streamwise direction between x/H values of 1 and 7, region where the leading-edge of the shock-train was expected to be found. The maximum y^+ turned out to be approximately 40, which required the use of wall-functions.

Figure 20 shows the Mach contours for the initial half of the domain (note the vertical scale is twice the horizontal, for purposes of clarity). The asymmetry has taken place, and several pairs of oblique shocks are visible. The flow is attached to the bottom and separated from the top as in the experiment, but this is entirely fortuitous; whether the flow separates on one surface or the other is entirely random.

The wall-pressure plots for the separated wall are plotted in figure 21. The location of the shock leading-edge is close to the experiment. The slope of the pressure rise, however, is underpredicted. Several factors may account for the disagreement. The most important may be the three-dimensional effects pointed before; corner effects may constraint the core flow, increasing the pressure gradient with respect to two-dimensional flows. Replacing the diffuser with a uniform back-pressure could also have an effect.

In the same figure, results are shown for a half-height domain with a symmetry boundary-condition at the center-line. As before, the extent of the upstream interaction is considerably smaller and gives a much-poorer agreement with the data.

The effects of grid resolution can be seen in figure 22. The medium grid corresponds to the baseline grid described before. The dimensions of the coarse and fine grids differ from the medium by a factor of two in each coordinate direction. The difference between the medium and fine grid appears small enough (and much smaller than between coarse and medium) to suggest grid convergence.

6. Conclusions

A series of numerical test cases was conducted to study the behavior of flows with upstream interaction. In particular, the possibility of obtaining a basic symmetric solution under conditions of symmetry in geometry, boundary conditions and grid was examined. With the usual numerical schemes, it was found impossible to obtain a basic symmetric solution. The results showed that the presence of large separated-flow regions interacting with shock-trains create non-symmetric perturbations that are greater than machine-zero. These perturbations, when coupled with the strong compression characteristic of flows with upstream interaction, may bring about the loss of the symmetry in the flowfield. The extent of departure from symmetry appears to be a function of the flow-blockage produced by the separation itself. The larger the asymmetry, the longer the extent of the upstream interaction compared to a symmetry-imposed calculation.

If the above is true, it may have an impact in some practical applications. Operational configurations, such as actual scramjet engines, are characterized by large aspect-ratio sections. Therefore, the modeling of half of the section with a symmetry boundary condition at the vertical symmetry plane is probably adequate. For small aspect-ratio sections (used in most experimental configurations) the use of any symmetry assumption is more problematical. The critical aspect ratio has yet to be determined.

An attempt was made to simulate the only experiment known to the author that displayed non-symmetric behavior in a flow with upstream interaction. The results were able to capture the qualitative behavior of the experiment. Quantitative comparison probably suffered from the use of a two-dimensional assumption to model a low aspect-ratio three-dimensional flow. A full three-dimensional simulation may be needed to determine the correlation, if any, between physical and numerical asymmetry. From the previous conclusions, the full cross-section may have to be

modeled.

It would also be instructive to study the stability of flows with upstream interaction within annular ducts. Experimental evidence[11][12] suggests that geometrically-axisymmetric flows remain fairly symmetric in the presence of upstream interaction. Whether their three-dimensional, full-section simulation also displays any symmetry remains to be determined.

References

[1] Rodriguez, C.G., White, J.A., and Riggins, D.W., "Three-Dimensional Effects in the Modeling of Dual-Mode Combustors", AIAA Paper 2000-3704, 36th AIAA/ASME/SAE/ASEE Joint Propulsion Conference and Exhibit, Huntsville, AL, 17-19 July 2000.

[2] Mohieldin, T., Olynciw, M., and Tiwari, S., "Asymmetric Flow-Structures in Dual Mode Scramjet Combustors with Significant Upstream Interaction", Report HX-835, NASA Langley Research Center, Hampton, VA, August 2000.

[3] Heiser, W.H., and Pratt, D.T., *Hypersonic Airbreathing Propulsion*, AIAA Educational Series, 1993.

[4] Carroll, B.F., "A Numerical and Experimental Investigation of Multiple Shock Wave/Turbulent Boundary-Layer Interactions in Rectangular Ducts", Ph.D. thesis, Mechanical and Industrial Engineering Dept., University of Illinois at Urbana-Champaign, Urbana, Illinois, 1988.

[5] Carroll, B.F., and Dutton, J.C., "Characteristics of Multiple Shock Wave/Turbulent Boundary-Layer Interactions in Rectangular Ducts", *Journal of Propulsion and Power*, Vol. 6, No. 2, March-April 1990, pp.186-193.

[6] Levy, Y., Hesselink, L., and Degani, D., "Anomalous Asymmetries in Flows Generated by Algorithms that Fail to Conserve Symmetry", *AIAA Journal*, Vol. 33, No. 6, June 1995, pp. 999-1007.

[7] Pulliam, T.H., and Chaussee, D.S., "A Diagonal Form of an Implicit Approximate-Factorization Algorithm", *Journal of Computational Physics*, Vol. 39, No. 2, 1981, pp. 347-363.

[8] White, J.A., and Morrison, J.H., "A Pseudo-Temporal Multi-Grid Relaxation Scheme for Solving the Parabolized Navier-Stokes Equations", AIAA Paper 99-3360, 1999.

[9] Edwards, J.R., "A Low-Diffusion Flux-Split Scheme for Navier-Stokes Calculations", *Computers and Fluids*, Vol. 26, No. 6, June 1997, pp. 635-659.

[10] Wilcox, D.C., *Turbulence Modeling for CFD, 2nd. Edition*, DCW Industries, 1998.

[11] Om, D., and Childs, M.E., "Multiple Transonic Shock-Wave/Turbulent Boundary-Layer Interaction in a Circular Duct", *AIAA Journal*, Vol. 23, No. 10, October 1985, pp. 1506-1511.

[12] Stockbridge, R.D., "Experimental Investigation of Shock Wave/Boundary Layer Interactions in an Annular Duct", *Journal of Propulsion and Power*, Vol. 5, No. 3, May-June 1989, pp. 346-352.

Figure 3: Convergent duct: Inviscid flow with RK integration.

Figure 1: Schematic of a rectangular duct with shock-train/boundary-layer interaction.
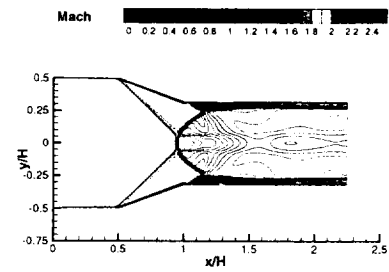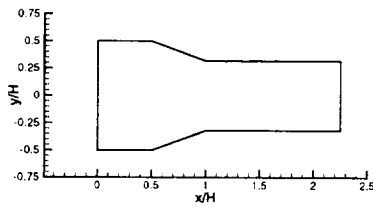
a)Mach Contours

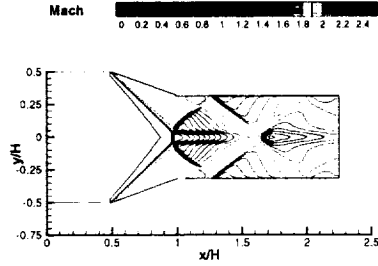Figure 2: Convergent duct: layout.

b) Vertical velocity at y = 0.
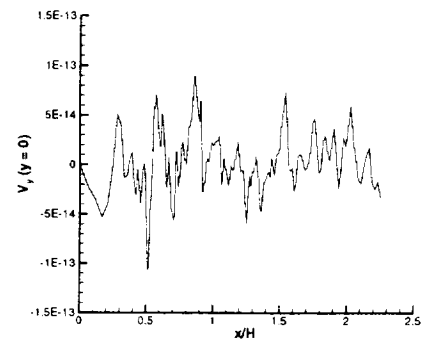
a)Mach Contours

Figure 4: Convergent duct: Viscous flow with RK integration.

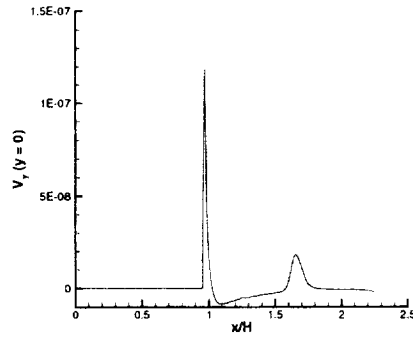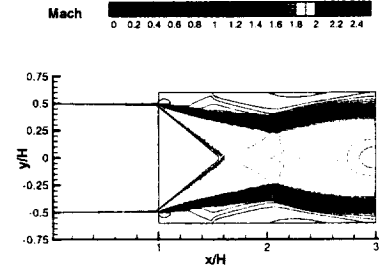a)Mach Contours
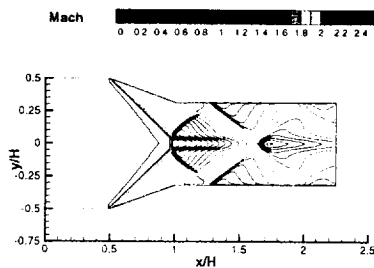
a)Mach Contours

b) Vertical velocity at y = 0.

b) Vertical velocity at y = 0.

Figure 5: Convergent duct: Inviscid flow with DAF integration.
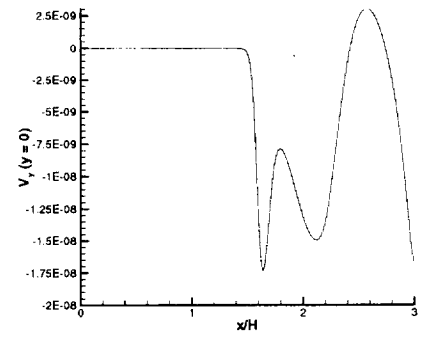
Figure 7: Sudden-expansion duct: p_{inj} = 40 KPa - RK integration.

a)Mach Contours
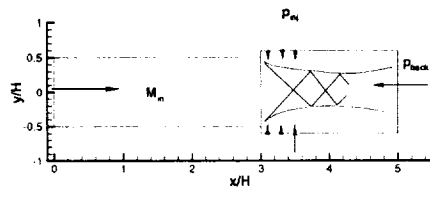
Figure 6: Sudden-expansion duct: layout.
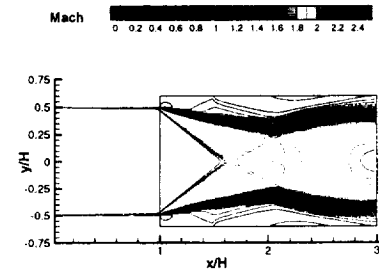
b) Vertical velocity at y = 0.
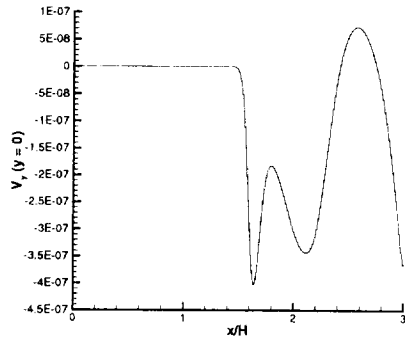
Figure 8: Sudden-expansion duct:
p_{inj} = 40 KPa - DAF integration.
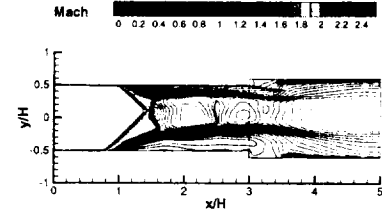
Figure 10: Sudden-expansion duct:
p_{inj} = 95 KPa - DAF integration.

a)Mach Contours

a) RK
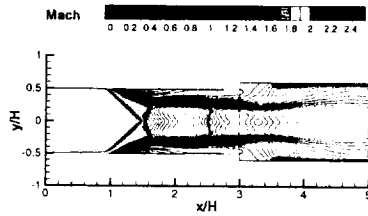
b) Vertical velocity at y = 0.

b) DAF

Figure 9: Sudden-expansion duct:
p_{inj} = 95 KPa - RK integration.
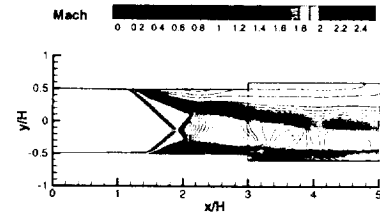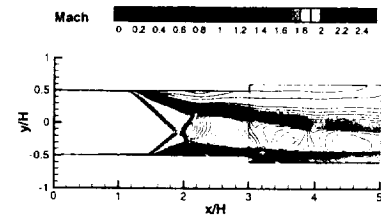
Figure 11: Sudden-expansion duct:
p_{back} = 80 KPa.

American Institute of Aeronautics and Astronautics
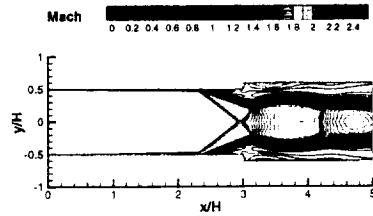
Figure 12: Sudden-expansion duct:
P_{back} = 80 KPa - Symmetry assumption.

b) Horizontal symmetry-plane

Figure 15: 3-D isolator: Symmetry planes.

Figure 13: 3-D isolator: layout.

Figure 14: 3-D isolator: Overall flowfield.
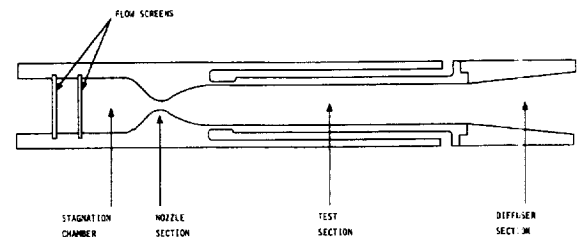
Figure 16: Experimental test-case:
Layout of the facility (courtesy B.F. Carroll).

Figure 17: Experimental test-case:
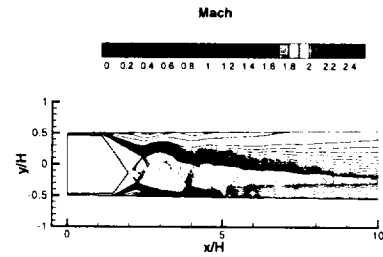Oil and schlieren visualizations
(courtesy B.F. Carroll).
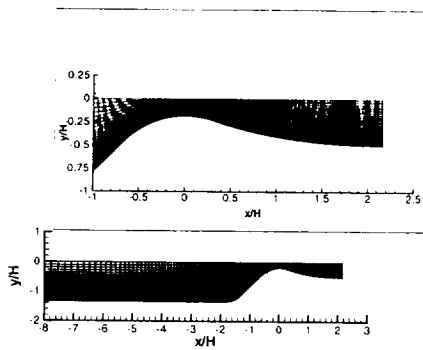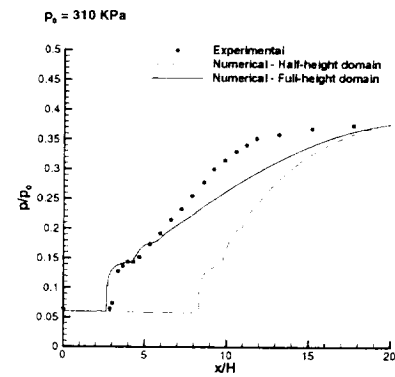

Figure 18: Experimental test-case:
Stagnation and nozzle section grid.

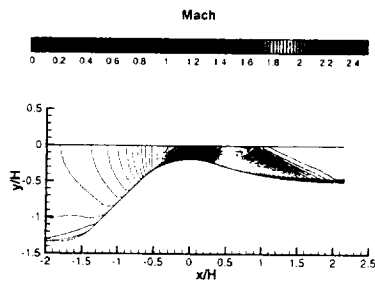Figure 19: Experimental test-case:
Stagnation and nozzle section Mach contours.

Figure 20: Experimental test-case:
Test-section Mach contours.

Figure 21: Experimental test-case:
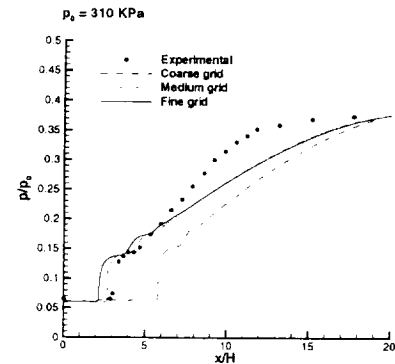Test-section wall pressures - Baseline grid.

Figure 22: Experimental test-case:
Test-section wall pressures - Grid resolution.